SIMULATION OF OLD SUPERNOVA REMNANTS BY MAGNETOHYDRODYNAMIC WAVE FRONTS

Y. SOFUE*
Max-Planck-Institut für Radioastronomie, Auf dem Hügel 69,
5300 Bonn 1, Germany

* A. von Humboldt Fellow on leave from Department of Physics Nagoya University, Nagoya, Japan

ABSTRACT

The three-dimensional behavior of expanding shells of old supernova remnants (SNR) in inhomogeneous interstellar medium is simulated by magnetohydrodynamic (MHD) wave fronts. The wave front undergoes strong refraction and reflection by the interstellar clouds. Subsequent focusing of the waves produces filamentary structures and bright patches. If the cloud size is comparable with or greater than the shell size, the SNR becomes greatly deformed from a sphere. Morphological features of a typical old SNR, S147, are fit reasonably well by a model which postulates interaction with several clouds of radii 8-12 pc.

1. INTRODUCTION

Old supernova remnants are characterized by their shell structures. They are observed to deviate from a circular shape and show complicated morphology composed of arc filaments. This fact suggests strong interactions of the shells with an inhomogeneous interstellar medium. To study such structures some two-dimensional models have been proposed (Sgro 1975; McKee and Cowie 1975; Chevalier and Gardner 1974). However, the existing models seem too simple to reproduce the highly structured features, which must require an understanding of the three-dimensional case.

In present paper the expanding SNR shell is approximated by a

magnetohydrodynamic (MHD) wave front, and its three-dimensional behavior in the inhomogeneous interstellar medium is examined.

2. MHD WAVES IN INTERSTELLAR SPACE

Simple computations of a spherical shock wave to simulate a SNR (e.g. Cox 1972) show that the expansion velocity of SNR at a radius $r \gtrsim 30$ pc decreases to 50 km/s or less, which is comparable with the Alfven velocity in the intercloud space ($\sim$ 40 km/s; see the estimation below). SNR like S147 may be in this stage. The SNR shock front in this stage will excite the fast-mode MHD waves, which are compression waves with the highest propagation velocity of all modes in the interstellar space. We assume here simply that the kinetic energy of the shell is converted into a MHD blast wave of fast mode at $r \gtrsim 20$-30 pc; namely we approximate the SNR shell by the MHD blast wave.

The propagation of the MHD wave is independent of the magnetic field configuration, and depends only on the distribution of the magnitude of Alfven velocity (Uchida 1970). This approximation is valid when the square of Alfven velocity, V^2, is much greater than that of sound velocity, c_s^2, or $(V/c_s)^2 \gg 1$. In the intercloud space we have the gas density $n = n_o = 0.05$-0.1 cm^{-3} and magnetic fields $B = B_o \approx 4\times10^{-6}$ gauss (Spitzer 1968; Heiles 1976), which yields $V = V_o \approx 40$ km/s. Since the sound velocity is $c_s \approx 10$ km/s, we have $(V/c_s)^2 \approx 16$. For typical HI clouds the values are: $n \approx 10$ cm^{-3}, $B \approx 20\times10^{-6}$ gauss, $c_s \approx 1$ km/s, yielding $(V/c_s)^2 \approx 200$. Thus in both cases the above condition is satisfied.

The equations describing the propagation of a MHD wave packet of small amplitude are written as follows (Uchida 1970):

$$\frac{dr}{dt} = V p_r / p, \tag{1}$$

$$\frac{d\theta}{dt} = V p_\theta / rp, \tag{2}$$

$$\frac{d\phi}{dt} = V p_\phi / rp \sin\theta, \tag{3}$$

$$\frac{dp_r}{dt} = -\frac{\partial V}{\partial r} + \frac{V}{rp}(p_\theta^2 + p_\phi^2), \tag{4}$$

$$\frac{dp_\theta}{dt} = -\frac{p}{r}\frac{V}{\partial\theta} - \frac{V}{rp}(p_\theta p_r - p_\phi^2 \cot\theta), \tag{5}$$

$$\frac{dp_\phi}{dt} = -\frac{p}{\sin\theta}\frac{V}{\partial\phi} - \frac{V}{rp}(p_\phi p_r + p_\phi p_\theta \cot\theta), \tag{6}$$

where $V = V(x, y, z) = V(r, \theta, \rho)$ is the Alfven velocity, the

vector $\mathbb{p} = (p_r, p_\theta, p_\phi)$ is defined through a phase function or an eikonal, Φ, as $\mathbb{p} = \text{grad}\,\Phi$ with $p = |\mathbb{p}|$, and $(x, y, z) = (r, \theta, \phi)$ are the cartesian and spherical coordinates of the packet.

For the spatial distribution of Alfven velocity we assume the following form:

$$V = V_o \left[1 + \Sigma_i \varepsilon_i \exp \left\{ - \frac{(X-X_i)^2}{\sigma_{X_i}^2} - \frac{(Y-Y_i)^2}{\sigma_{Y_i}^2} - \frac{(Z-Z_i)^2}{\sigma_{Z_i}^2} \right\} \right] \quad (7)$$

Here the position of the i-th cloud is denoted by (x_i, y_i, z_i) and its extend in the x, y, and z directions by $(\sigma_{x_i}, \sigma_{y_i}, \sigma_{z_i})$. Enhancement of the Alfven velocity in the cloud is represented by ε_i: if $\varepsilon > 0$ the velocity increases toward the cloud center and the cloud is regarded as "concave lens", where the waves are reflected outward. If $\varepsilon < 0$, the cloud is a "convex lens", into which the waves focus.

We now integrate equations (1)-(6) for the above V distribution. As an initial condition at t=0 of computation, we distribute MHD wave packets on a small sphere centered at (x, y, z) = (0, 0, 0). Each wave packet is initially given a constant radial velocity.

3. FORMATION OF FILAMENTARY STRUCTURES AND BRIGHT KNOTS

The computed results are displayed in the form of mesh surfaces (Figure 1-4), where each mesh point represents the position of a wave packet.

i) Filaments of thin sheets seen edge-on: Figure 1 shows an evolution of a MHD wave front encountering a cloud with low Alfven velocity. The waves suffer strong refraction due to the cloud and the front is corrugated to form a concave surface. In this concave front, the energy flux of the waves is higher than in the surrounding regions. When this feature appears near the limb of a SNR, we can observe a sharp filament as a result of an edge-on view of the corrugated front as seen in the lower diagrams of Figure 1.

This sort of filament, which is not a true filament but a projection effect of the curved sheet, is characterized by the fact that its center of curvature is on the outward side of the sheet, that is, away from the center of the SNR. A long, strong filament near the southern limb of S 147 may be a typical example of this ge-on sheet filament.

ii) Bright Knots: If the Alfven velocity in the cloud is much smaller than that of the sourrounding region, the rays strongly focus on the central region of the cloud. As shown in the later stage of Figure 1, the MHD waves form there a deeply concave front of high energy flux density. The focal region illuminated by the refracted rays will appear as a bright knot.

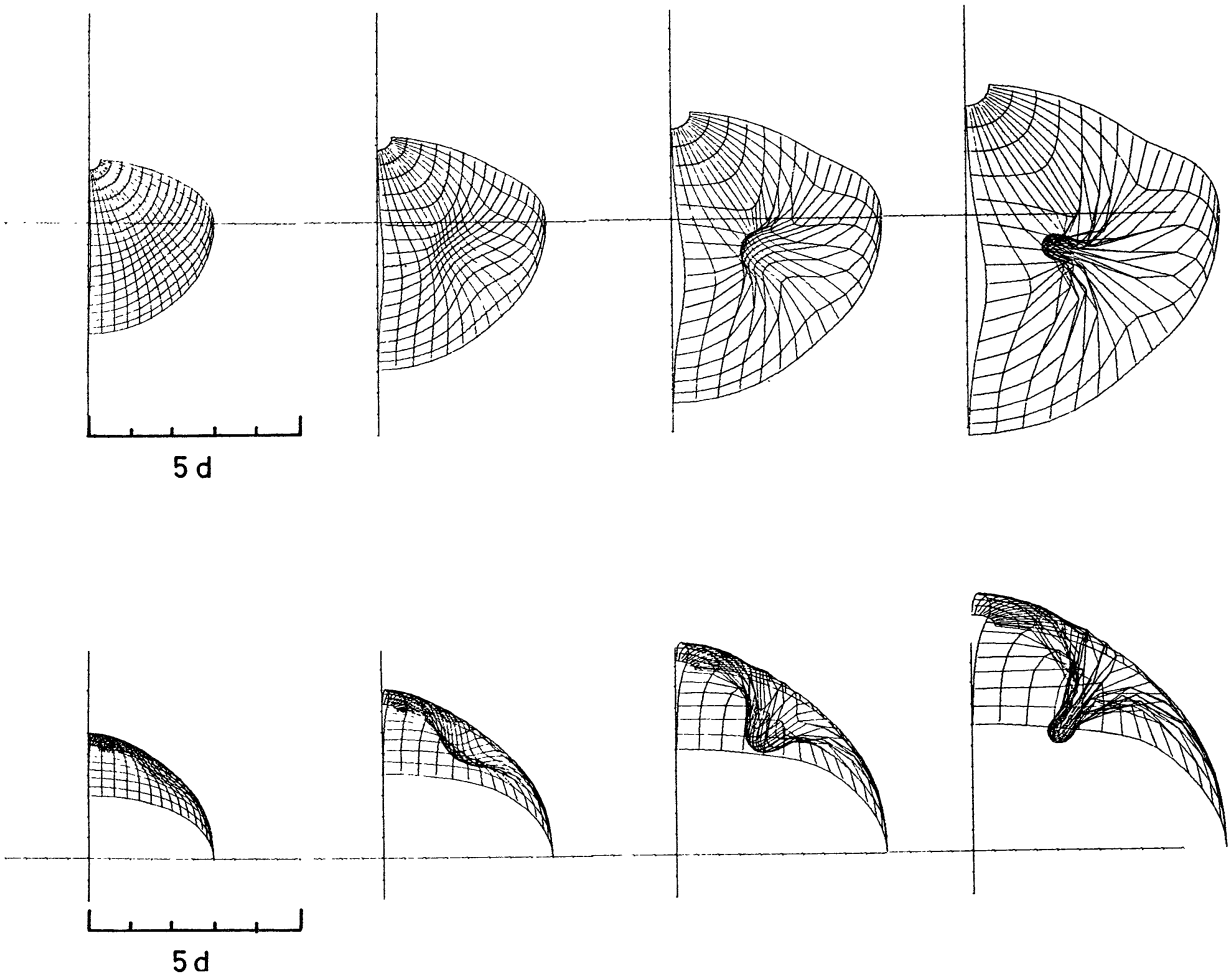

Fig.1: MHD wave front encountering a spherical low-V cloud with $\varepsilon = -0.95$ located at (x, y, z) = (2d, 2d, 2d) and $\tau = 1d$. The upper diagrams show the views from a line of sight at an angle of 60° to the x-y plane; the lower diagrams show edge-on views. The time interval is $\tau = d/V_o$. A filamentary structure is simulated by a projection of a corrugated surface which has been focussed by the cloud. As the front expands further, a bright patch appears with a high wave density. (d: normalizing factor of length)

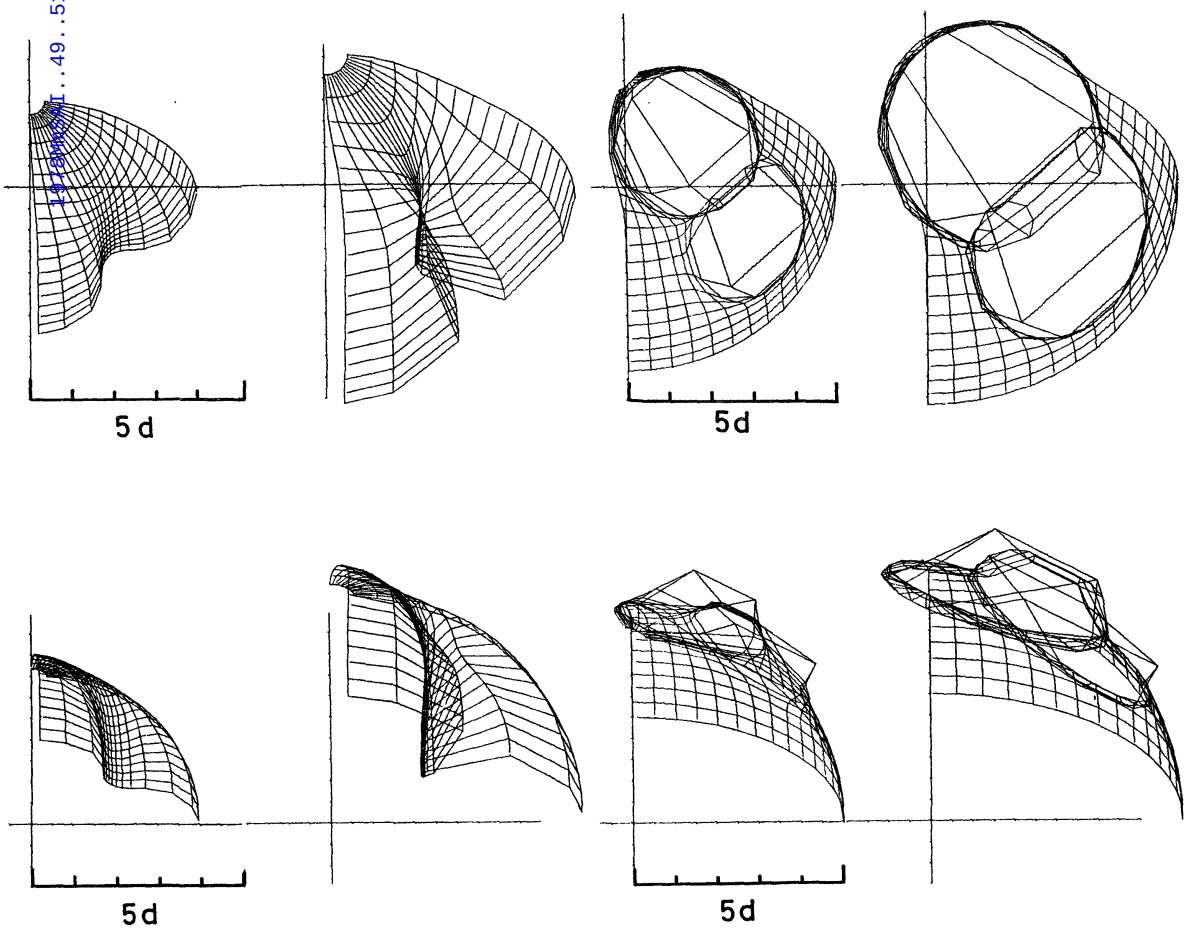

Fig. 2: The same as Fig. 1 except that the cloud is elongated in the z-direction; (σ_x, σ_y, σ_z) = (1d, 1d, 5d). The rays focussing along the axis of the cloud form a filamentary structure extending in the z-direction.

Fig. 3: MHD wave front encountering two high-V clouds (ε = 2) of the same scale; ε = 1d located at (x, y, z) = 1.5d, 1.5d, 4.7d) and (3d, 3d, 3d). Some complicated filaments with arc structures appear.

iii) Long, straight filaments: Figure 2 shows a front encountering a low-V cloud elongated in the z-direction. In this case, a long string of focussing waves appears along the major axis of the cloud. The Cygnus Loop has a long, wavy filament across the central region, which might be understood in the present model.

iv) Arc-String Filament: When the MHD front encoutners a high-V cloud, the rays are reflected outward. Figure 3 shows the behavior of a front against two clouds of high Alfven velocity. The rays are reflected near the surface of the clouds, and converge to produce thin and sharp focal rings of high energy flux density, which will be observed as arc filaments. This type of filament is a "true" filament, or a string, and should be distinguished from the edge-on sheet filament in section i). This sort of string is not necessarily associated with the outer limb, but can appear anywhere on the SNR shell. A typical example may be the sharp and thin arc in the southern quadrant of S147 near its center. (See, e.g., photographs by van den Bergh et al. 1973).

4. LARGE-SCALE DEFORMATION OF A SNR SHELL

In addition to the filaments and bright knots, old SNRs usually show a large scale deformation from a circular shell. This may be easily understood as a result of the interaction with larger-scale irregularities. To examine the influence of such large-scale inhomogeneities, we calculate the following two cases: i) the MHD waves encounter large-scale clouds; ii) the MHD front expands into a plane-stratified medium. The latter presumes the influence of the galactic gas layer on very old SNRs.

i) Large Clouds: Figure 4 shows the case of an encounter with two clouds with $\varepsilon = 1$ and radius = 2d located at (x, y, z) =(2d, 2d, 2d) and (2d, 2d, -2d) respectively. The shell is so strongly deformed that the half of the shell facing the clouds practically disappears. As a consequence an incomplete arc structure remains on the opposite side of the clouds. We suggest that VRO 420501, RCW86, and CTB1 may be typical examples of SNRs which have been deformed in such a manner. A large scale deformation of the south-western part of IC 443 may be also explained in this manner.

ii) Plane-Stratified Disk: If we assume that the gas density and magnetic pressure in the galactic plane are distributed as a whole plane parallel in the form of exp $(-z^2/h_g^2)$ and exp $(-z^2/h_m^2)$, respectively, the Alfven velocity is expressed as $V = V_o \exp(z^2/H^2)$, where z is the distance from the galactic plane. H is given by $H = h_g h_m/(h_m^2-h_g^2)^{1/2}$ since $h_g < h_m$ in the Galaxy (Sofue 1976).

We now examine the behavior of the MHD front in the plane-stratified disk. The galactic effect will be especially significant if the SNR is old enough with large radius and its location is high above the galactic plane. Figure 5 shows the behavior of the ray paths and fronts in the x-z plane for the case that the SNR

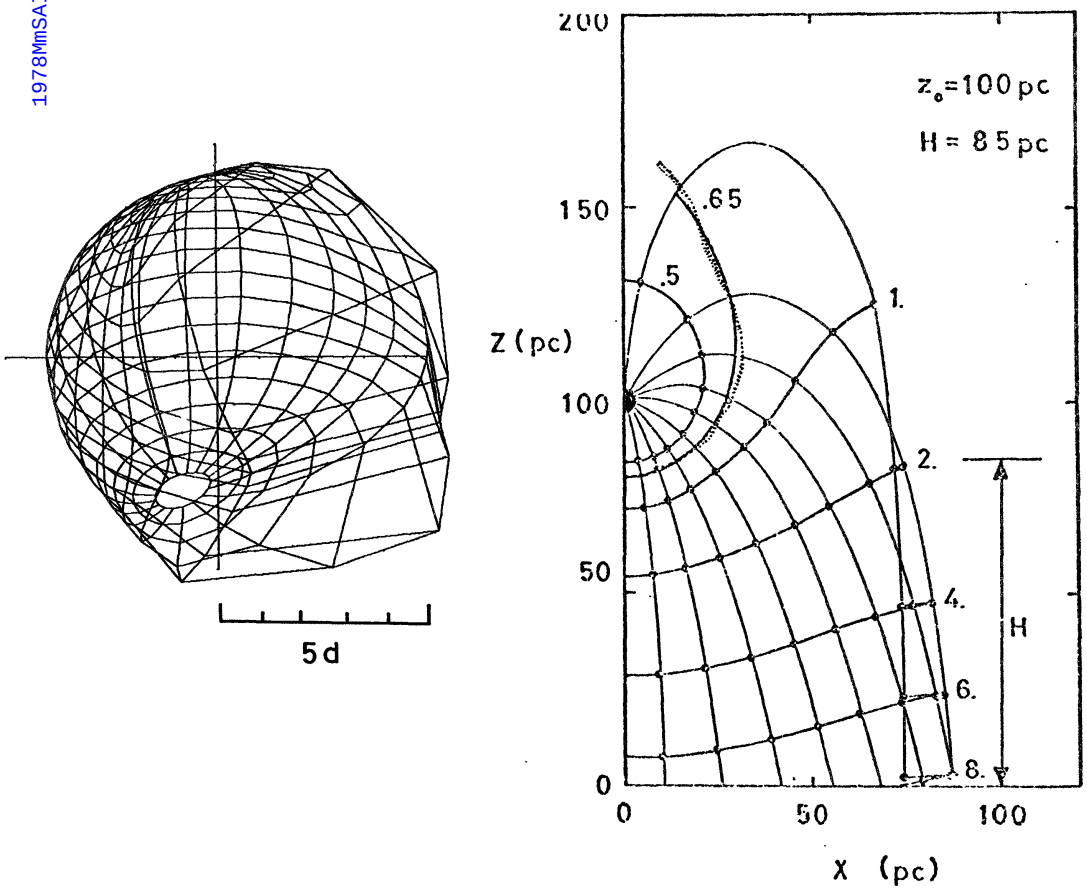

Fig. 4: An expanding MHD shell encountering two large clouds of high Alfven velocity (ε = 1); (x, y, z) =(2d, 2d, 2d) and (2d, 2d, -2d) with σ = 2d. Strong deformation from a sphere occurs, which resembles some old SNRs like as CTB 1 and IC 443.

Fig. 5: Propagation of MHD waves in a plane-stratified galactic disk where the Alfven velocity varies as $V=V_o \exp(z^2/H^2)$ with H = 85 pc. Thick lines are wave front, thin lines ray paths. This figure simulates the evolution of SNR G65.2 + 5.7 in Cygnus which is assumed to have exploded at a height of z_o = 100 pc above the galactic plane (dotted line).

explosion takes place at a height of z_o = 100 pc above the galactic plane. Here we assumed that H = 85 pc. In the initial stage of the expansion, the shell remains almost spherical. If the radius exceeds $\sim$ 30 pc, however, the front is strongly affected by the steep z-variation of the Alfven velocity: the upper part of the shell opens suddenly to form a dish-like surface.

A typical example of such high-z, old SNR will be the SNR G65.2+5.7 in Cygnus (Gull et al. 1977; see also the contribution by Sofue et al. in this volume). The dotted line in Figure 5 is a sketch of geometrical feature of this SNR taken from a deep photograph at OIII line by Gull et al. Here we assume the distance to this SNR to be 1 kpc. The open configuration and elongated feature toward the high-z region are well fitted by a certain stage of the computed MHD front.

We see that a SNR can hardly retain a spherical shell and is almost completely broken up if its radius exceeds $\sim$ 50 pc. In this context it is of interest to note that some galactic spurs, Loops I-IV, of radio continuum have been suggested to be very old SNRs with radii $\sim$ 100 pc or more. However, we must conclude that it is quite difficult for SNR shells to remain in a loop structure in such an extremely late stage.

5. APPLICATION TO THE SUPERNOVA REMNANT S147

S147 is a typical old SNR, well known for its beautiful shape, rich in long and delicate filaments. We here try to reproduce the geometrical features of S147 by assuming the existence of a few interstellar clouds in and around the SNR. We assume the radius of S147 to be 35 pc (Downes 1971). In Figure 6 we illustrate the spatial distribution of the clouds and their extents in the coordinate system used in the computation. Table 1 gives the Alfven velocities for individual clouds which have been adopted by trial and error so that the result fits reasonably well the apparent orientations of filaments and bright knots.

Figure 7 shows the computed result. Some characteristic features are reproduced: a prominent long filament near the southern limb which is an edge-on sheet filament due to an elongated low-V cloud No.1; a bright knot in the EN quadrant as a result of focussing by the very low-V cloud No.2; large-scale deformations of the shell toward the east and west, which are caused by high-V clouds of larger scale (Nos. 3 and 4). (Compare with the photograph of S147 in the atlas by van den Bergh et al. (1973))

We see that the cloud diameters are required to be around 20 pc, which agrees satisfactorily with the typical diameter of the "standard" HI cloud (Spitzer 1968). The present method provides therefore information about such quantities as sizes, densities, magnetic fields and the three-dimensional distribution of the clouds: that is, the old supernova remnants can be used as inter-

Table 1: Alfven velocities adopted for the clouds in S147 and corresponding magnetic fields for some assumed gas densties.

Cloud No.	V km/s	n = 1	10	100 cm^{-3}
1	4	B=1.8 10^{-6}	5.6 10^{-6}	1.8 10^{-5} gauss
2	2	0.9 10^{-6}	2.8 10^{-6}	8.8 10^{-6}
3	80	3.6 10^{-5}	1.1 10^{-4}	3.6 10^{-4}
4	120	5.4 10^{-5}	1.7 10^{-4}	5.4 10^{-4}
5	64	2.8 10^{-5}	9.2 10^{-5}	2.8 10^{-4}

Assumed intercloud values: n_o = 0.05 cm^{-3}, B_o = 4 10^{-6} gauss, V_o = 40 km/s.

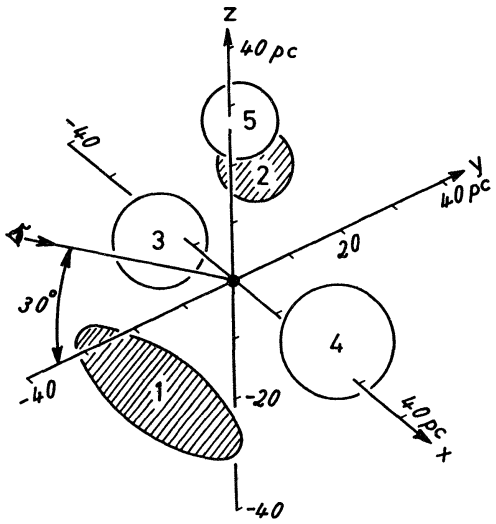

Fig. 6: Spatial distribution of interstellar clouds around the center of the SNR, S147. Shaded clouds have low Alfven velocities; unshaded clouds have high Alfven velocities. The coordinate system is chosen so that the line of sight is in the y-z plane and at 30° with the x-y plane. The SNR center is at the origin. See also Table 1.

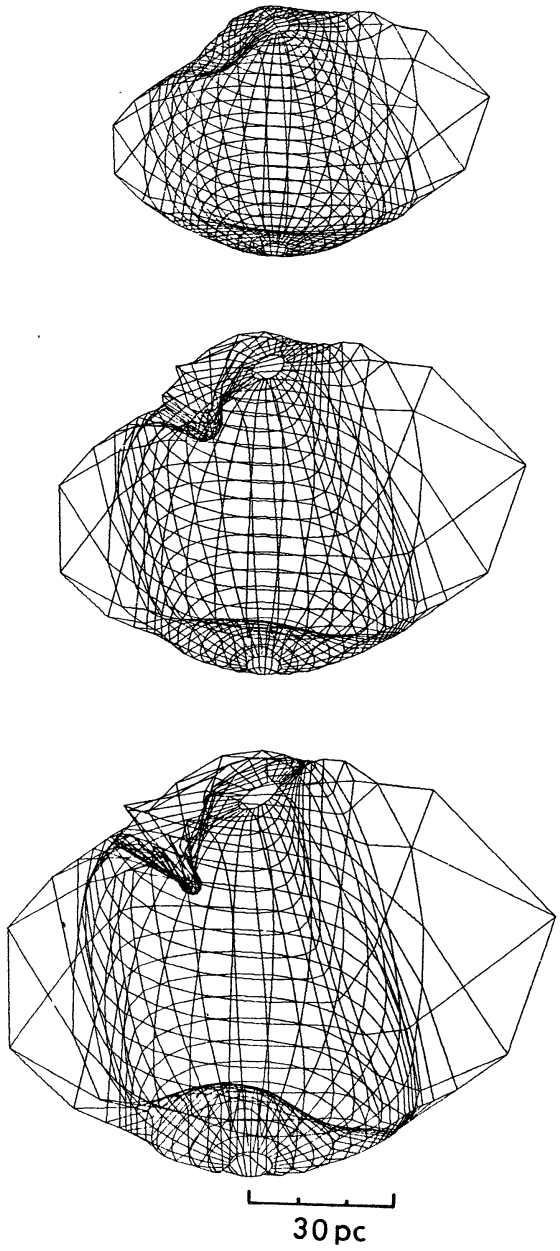

Fig. 7: Simulation of the SNR S147 under the influence of several interstellar clouds, whose parameters are given in Table 1 and Fig. 6. The second figure corresponds to the present S147. Note a reproduction of some characteristic features as filament near the southern limb, protuberances in the E and W sides, and a bright patch in the NE quadrant. (N to the top; E to the left).

stellar probes to get such quantities. In Table 1 we give magnetic field strengths in the clouds in S147 for assumed densities of n = 1, 10 and 100 cm^{-3}, where the ambient values are assumed to be as n_o = 0.05 and B_o = 4x10^{-6} gauss, or V_o = 40 km/s.

6. COMMENTS

The MHD wave front strongly focusses on the central region of a cloud with low Alfven velocity, which will result in a rapid increase of the amplitude growing into a strong shock wave, similar to a spherical implosion. If the time scale of cooling of the gas is shorter than the time taken for the shock to propagate through the cloud, the strong compression by the focussing wave will enhance thermal instability followed by a gravitational fragmentation of the cloud into small denser clouds. Further contraction of the fragments will evolve into sites of star formation. It is therefore possible that star formation will be enhanced in Low-V interstellar clouds by the focussing of SNR shock front even if the SNR is very old.

On the other hand if the cooling is not rapid enough, the thermalization of the shock energy will heat up the cloud, increasing its internal pressure and the cloud may be evaporated through passage of the SNR shock.

This contribution is a summary of my paper which is in press for Astron. Astrophys. (Sofue 1978). See this paper for further discussions and references.

References

Chevalier, R.A. and Gardner, J. 1974, Astrophys. J. 192 457
Cox, D.P. 1972, Astrophys. J. 178, 159
Downes, D. 1971, Astron. J. 76, 305
Gull, T.R., Kirshner, R.P., Parker, R.A.R. 1977, Astrophys. J. 215 L69
Heiles, C. 1976, Ann. Rev. Astron. Ap. 14, 1
McKee, C.T., Cowie, L.L. 1975, Astrophys. J. 195, 715
Sgro, A. 1975, Astrophys. J. 197, 621
Sofue, Y. 1976, Astron. Astrophys. 48, 1
Sofue, Y. 1978, Astron. Astrophys. in press
Spitzer, L., Jr. 1968, in Stars and Stellar System VII; Nebulae and Interstellar Matter (Univ. Chicago Press), ed. Middlehurst and Aller, Chap. I
Uchida, Y. 1970 Publ. Astron. Soc. Japan 22, 341
van den Bergh, S., Marscher, A.P., Terzian, Y. 1973, Astrophys. J. Suppl. 26, 19